

ARTICLE

Intermolecular Hydrogen Bonds Formed Between Amino Acid Molecules in Aqueous Solution Investigated by Temperature-jump Nanosecond Time-resolved Transient Mid-IR Spectroscopy[†]

Man-ping Ye^{a,c}, Heng Li^{a,c}, Qing-li Zhang^{a,c}, Yu-xiang Weng^{a,c*}, Xiang-gang Qiu^{b,c}*a. Laboratory of Soft Matter Physics, Institute of Physics, Chinese Academy of Sciences, Beijing 100080, China;**b. Laboratory for Superconductivity, Institute of Physics, Chinese Academy of Sciences, Beijing 100080, China;**c. Beijing National Laboratory of Condensed Matter Physics, Beijing 100080, China*

(Dated: Received on June 3, 2007; Accepted on July 14, 2007)

Carboxyl (COO^-) vibrational modes of two amino acids histidine and glycine in D_2O solution were investigated by temperature-dependent FTIR spectroscopy and temperature-jump nanosecond time-resolved IR difference absorbance spectroscopy. The results show that hydrogen bonds are formed between amino acid molecules as well as between the amino acid molecule and the solvent molecules. The asymmetric vibrational frequency of COO^- around $1600\text{--}1610\text{ cm}^{-1}$ is blue shifted when raising temperature, indicating that the strength of the hydrogen bonds becomes weaker at higher temperature. Two bleaching peaks at 1604 and 1612 cm^{-1} were observed for histidine in response to a temperature jump from $10\text{ }^\circ\text{C}$ to $20\text{ }^\circ\text{C}$. The lower vibrational frequency at 1604 cm^{-1} is assigned to the chain COO^- group which forms the intermolecular hydrogen bond with NH_3^+ group, while the higher frequency at 1612 cm^{-1} is assigned to the end COO^- group forming hydrogen bonds with the solvent molecules. This is because that the hydrogen bonds in the former are expected to be stronger than the latter. In addition the intensities of these two bleaching peaks are almost the same. In contrast, only the lower frequency at 1604 cm^{-1} bleaching peak has been observed for glycine. The fact indicates that histidine molecules form a dimer-like intermolecular chain while glycine forms a relatively longer chain in the solution. The rising phase of the IR absorption kinetics in response to the temperature-jump detected at 1604 cm^{-1} for histidine is about $30\pm 10\text{ ns}$, within the resolution limit of our instrument, indicating that breaking or weakening the hydrogen bond is a very fast process.

Key words: Histidine, Glycine, 4-Methylimidazole, Hydrogen bonding, Temperature-jump, Time-resolved IR spectrum

I. INTRODUCTION

Hydrogen bonding is an important force in forming and maintaining the protein secondary and higher order structures. For example, the intermolecular or intramolecular β -sheet structure is formed by hydrogen bonding between carbonyl ($\text{C}=\text{O}$) groups with their counterpart NH groups. Hydrogen bonding also plays a key role in the solvation of protein surfaces. In spectroscopic study, hydrogen bonding can be investigated as a perturbation to the host molecules either on its electronic or vibrational spectra. The effect of hydrogen bonding on the IR spectrum of polypeptides has been studied in both theory and experiment [1,2]. As a result, hydrogen bonding formed in polypeptides would cause a red-shift of the $\text{C}=\text{O}$ vibration in amide I region. It has been reported that the main amide I frequency for poly- β -L-Ala is at 1632 cm^{-1} while that for poly- β -Glu is at 1624 cm^{-1} , such a difference in the amide I

frequency was interpreted as the formation of stronger hydrogen bonds in the latter [3]. For α -helices there is also evidence for an effect of hydrogen bonding on the vibrational frequency since solvated helices absorb approximately 20 cm^{-1} lower than non-solvated helices [4-6]. It has also been noted that the position of the amide I maximum absorbance of protein secondary structures correlates with the strength of the hydrogen bonding which decreases in the order of intermolecular extended chain ($1610\text{--}1628\text{ cm}^{-1}$), intramolecular antiparallel β -sheets ($1630\text{--}1640$), α -helices ($1648\text{--}1658\text{ cm}^{-1}$), 3_{10} - α -helices ($1660\text{--}1666\text{ cm}^{-1}$) and non-hydrogen bonded amide groups in DMSO ($1660\text{--}1665\text{ cm}^{-1}$) [7]. Therefore the vibrational spectra of protein functional groups such as backbone $\text{C}=\text{O}$ and amino acid side chain are valuable reporters for the protein secondary structures and environment of the proteins [8], which enables IR spectroscopy a powerful tool in the study of protein secondary structures.

However, it has been reported that the IR spectrum of protein is sensitive to its environment such as pH and salt effect [9], which makes it difficult in assignment of the vibration spectrum. The laser-induced temperature-jump method combined with the time-resolved infrared spectroscopy is well established for

[†]Part of the special issue "Cun-hao Zhang Festschrift".

*Author to whom correspondence should be addressed. E-mail: yxweng@aphy.iphy.ac.cn

the study of ultrafast protein folding/unfolding dynamics [10,11]. The T-jump method provides a means to quickly perturb the equilibrium position of the ensemble of possible states. The relaxation to the new equilibrium point corresponding to the elevated temperature is monitored by time-resolved infrared spectroscopy. This paper reports a temperature-jump (T-jump) time-resolved transient mid-IR spectroscopic study of thermally-induced hydrogen bond breaking and weakening in amino acid aqueous solution, in which histidine and glycine were chosen as the samples.

Histidine has an imidazole group as a side chain having two nitrogen atoms which can be protonated or deprotonated [12] and functions as a competent proton transfer mediator in various proteins [13]. Histidine also serves as both a hydrogen-bond donor and an acceptor [14], and this hydrogen bonding property is of importance in proton transfer reactions [15] and in organizing the active centers of enzymes. Glycine is the simplest amino acid and selected for comparative study. Both of the amino acids form either intermolecular hydrogen bonds or hydrogen bonds with the solvent molecules. Temperature jump was used to break the hydrogen bonds or reduce the strength of the hydrogen bonds. The corresponding hydrogen bonding effect on the vibrational spectra was detected by time-resolved IR transient difference absorbance spectra. Our results show that glycine can form a relatively longer intermolecular chain through the formation of hydrogen bonds, while histidine seems to form mainly a dimer-like structure.

II. MATERIALS AND METHODS

A. Chemicals

L-histidine and glycine were purchased from Wako Pure Chemical Industries, Ltd. 4-Methylimidazole (4-MeIm) was from Acros Organics. They were of the highest available grades and used without further purification. D₂O (D, 99.8%) was from Beijing Chemical factory. DCl (20%) in D₂O purchased from Cambridge Isotope Laboratories Inc. was used to adjust the *pD* value of D₂O.

B. FTIR spectroscopy

FTIR spectra were collected on an ABB-BOMEN FTIR spectrometer (ABB-BOMEM, Bureau, Québec) using a temperature controlled IR cell as described elsewhere [16]. The two-compartment IR cell contained both the sample and D₂O between CaF₂ windows with a 56 μm spacer. Temperature regulation was controlled by a water bath (Haake K30) at an accuracy of ± 0.25 °C. To correct for slow instrument drift, a programmable translation stage was used to move both

the sample and reference cells in and out of the infrared beam alternatively. To eliminate spectral interference from atmospheric water vapor, the measurement was performed in a vacuum chamber at a vacuum of 22 Pa in a specially designed chamber which allows the water flowing through vacuum-sealed pipes to maintain the samples at the desired temperature.

For both static and time-resolved IR measurements, the corresponding amino acid solutions were prepared by directly dissolving the solids in D₂O in an airtight bottle for 24 h, and the final concentration was 560 mmol/L for static and 24 mmol/L for time-resolved IR measurement. During the temperature-dependent FTIR measurement, the spectra were taken about every 5 °C between 4 and 90 °C after the sample was thermally equilibrated for 15 min at each temperature. The corresponding reference D₂O spectra were recorded under the same condition.

C. T-jump and time-resolved IR difference absorbance spectra

The laser induced T-jump technique and the time-resolved IR spectrometer have been described elsewhere [16,17]. Briefly, a 1.9 μm pulsed laser with a pulse width of 10 ns was used to heat the solution rapidly known as temperature jump. The T-jump pulse was generated by Raman shifting a Nd:YAG laser (Lab 170, 10 Hz, 8-12 ns, Spectrum Physics) fundamental at 1064 nm in a Raman cell filled of H₂ gas at a pressure about 5.0 MPa.

A liquid N₂ cooled CW CO laser (Dalian University of Technology) was employed as the IR probe source, which was tunable from 5.0 μm (2000 cm^{-1}) to 6.5 μm (1540 cm^{-1}). A single output wavelength can be selected within the CO vibration-rotation spectrum with an approximate spectral spacing of 4 cm^{-1} . The probe beam was focused at the center of the heated volume. Probing only the center of the heated volume ensures a uniform temperature distribution in the probe volume by avoiding the temperature gradient produced on the wings of the Gaussian pump beam [18]. A T-jump of 10-15 °C can be obtained routinely in an approximately 25 nL laser interaction volume (0.8 mm spot size \times 0.05 mm path length).

The transient transmission of the probe beam through the sample was detected by a liquid N₂ cooled photovoltaic MCT detector (Kolmar, MA, USA) equipped with a sensitive current preamplifier (Kolmar, KA020-A1) which has a band pass of 20 MHz. The temporal resolution of the time-resolved IR difference absorption signal has a limit about 20 ns (limited by the detector rise time and laser pulse width, after deconvolution of the instrumental response function). The intensities of the transmitted probe IR beam and the corresponding transient absorbance change induced by the T-jump pulses represented by V_0 and ΔV respectively were recorded by a digital oscilloscope (Tektronix

TDS520D). Both the signals were finally transferred to a PC for data analysis. Instrument control and data collection programs were written in LabVIEW. The T-jump time-resolved IR absorbance difference spectra were reconstructed from the kinetics measurement at various wavelengths.

In static FTIR measurements, a sample cell with dual compartments was used to allow the separate measurements of the sample and reference (D_2O) under almost identical conditions. The temperature-dependent FTIR spectra of D_2O were employed as an internal standard for T-jump calibration. The calibration of the T-jump amplitude follows the reported protocols [19]. Briefly, the T-jump induced absorbance change of the reference D_2O at probing wavelength ν ($\Delta A(\Delta T, \nu)$) was measured, and the T-jump amplitude was found by the following equation:

$$\Delta A(\Delta T, \nu) = a(\nu)\Delta T + b(\nu)\Delta T^2 \quad (1)$$

where $\Delta T = T_f - T_i$ is the T jump amplitude; T_f and T_i correspond to the final and initial temperature, respectively; and $a(\nu)$ and $b(\nu)$ are the fitting parameters determined by the FTIR spectra of D_2O measured at different temperatures [20].

The instrumental temporal response of this system is about 80 ns as determined by fitting the T-jump kinetics of the D_2O reference signal convoluted with a Gaussian instrumental response function, where the rising time constant for heating D_2O is set as 20 ns based on the pulse width of the Nd:YAG laser. If it is not stated otherwise, the time constants from fitting of the experimental kinetics are deconvolved by the instrumental response function.

III. RESULTS AND DISCUSSION

Histidine has three functional groups, i.e., carboxylic, amino and imidazole groups, all the three functional groups contribute to its IR spectrum [21-23]. Thus FTIR spectra of histidine, glycine and 4-MeIm were acquired for comparison. The molecular structures of the three species are illustrated in Fig.1. Figure 2 shows the FTIR spectra of histidine, glycine, and 4-MeIm in D_2O . At the neutral pD , amino acids in aqueous solutions are zwitterionic, and all modes of the NH_3^+ group and COO^- group can be expected in line with literature data [24]. In Fig.2 no absorption bands appear in the spectral region 1710-1790 cm^{-1} , which indicates that the carboxylic groups ($COOH$) are deprotonated while the amino groups are protonated [25]. Figure 2 reveals two strong absorption bands located at 1621 and 1413 cm^{-1} for glycine, and 1617, 1407 cm^{-1} for histidine respectively. These two bands correspond well to those of asymmetric and symmetric stretching motion of the carboxyl group (COO^-) [26]. A major absorption at 1439 cm^{-1} is observed in the FTIR of 4-MeIm which also appears in that of glycine and histidine with a slight

difference in the peak position, it can be assigned to the CN stretching vibration and CH_3 deformation motion [25].

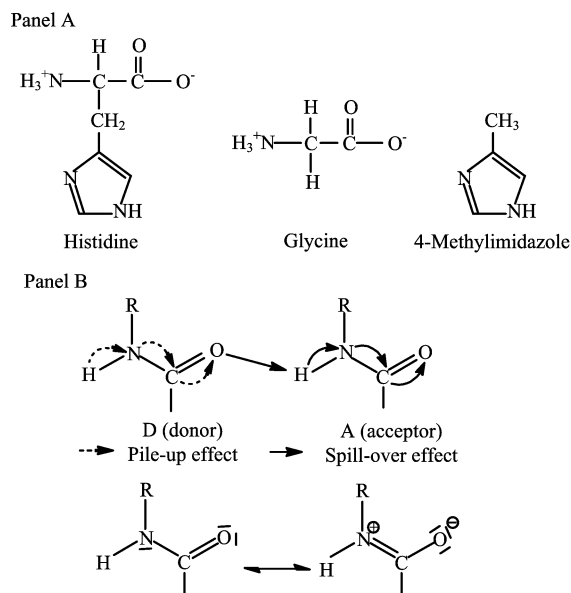


FIG. 1 Schematic diagrams for the molecular structures of histidine, glycine and 4-MeIm (Panel A); Panel B shows effect of intermolecular hydrogen bonding on the amide fundamentals.

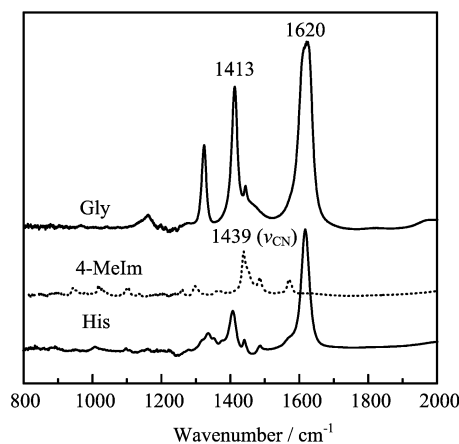


FIG. 2 Comparison of FTIR absorbance spectra of histidine, glycine and 4-MeIm in D_2O at the temperature of 25 $^{\circ}C$ in the amide I and amide II region. The middle and top spectra are on the same scale as the bottom one, but off-set along the y axis.

Temperature-dependent FTIR spectra of the three species in D_2O solution have been acquired in a wide range of temperatures ranging from 5 $^{\circ}C$ to 90 $^{\circ}C$ in a step of roughly 5 $^{\circ}C$. Figure 3(a) shows a set of carboxyl asymmetric vibrational spectra for histidine acquired at three typical temperatures, i.e., 5, 50, and 90 $^{\circ}C$, which indicates that the absorption band is blue-shifted from 1617 cm^{-1} at low temperature to 1620 cm^{-1} at high

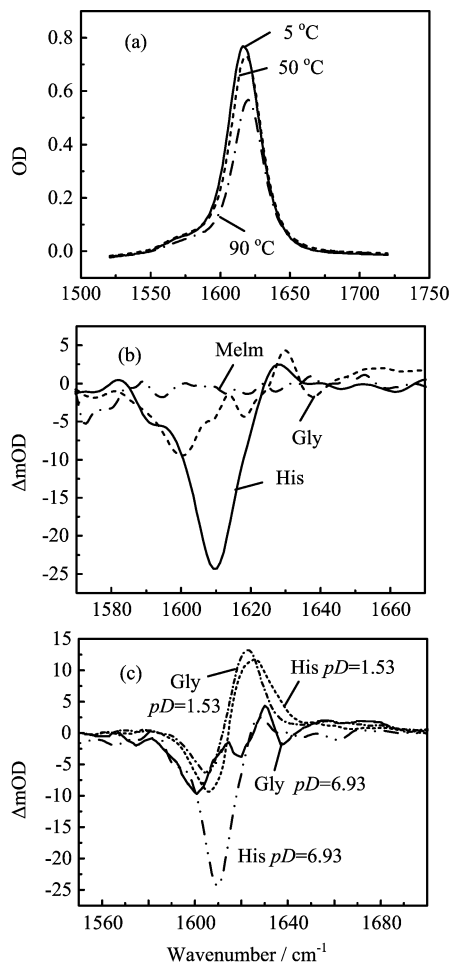


FIG. 3 (a) FTIR absorption spectra of carboxyl asymmetric vibration for histidine in D₂O at different temperatures of 5, 50 and 90 °C; (b) Comparison of FTIR absorbance difference spectra between 20 and 10 °C for histidine, glycine and 4-MeIm in D₂O in the spectral region of 1520-1720 cm⁻¹. (c) Comparison of FTIR absorbance difference spectra between 20 and 10 °C for histidine and glycine dissolved in D₂O with different acidity of *pD*=6.93 and *pD*=1.53.

temperature accompanied by an intensity loss. The shift of the absorption band to higher frequency and the weakening of the absorption band are primarily due to the broken or weakened hydrogen bonds. The same tendency has also been observed in glycine. Such a temperature-dependent peak shift can be more clearly illustrated by absorbance difference FTIR spectra at two different temperatures. Figure 3(b) presents the FTIR difference spectra of histidine, glycine and 4-MeIm between 20 and 10 °C. Figure 3(c) shows the FTIR absorbance difference spectra of glycine and histidine dissolved in D₂O with different acidity of *pD*=6.93 and *pD*=1.53 respectively between 20 and 10 °C.

To get an insight into the thermally induced change of histidine and glycine with their surrounding D₂O, T-jump time-resolved IR difference absorbance spec-

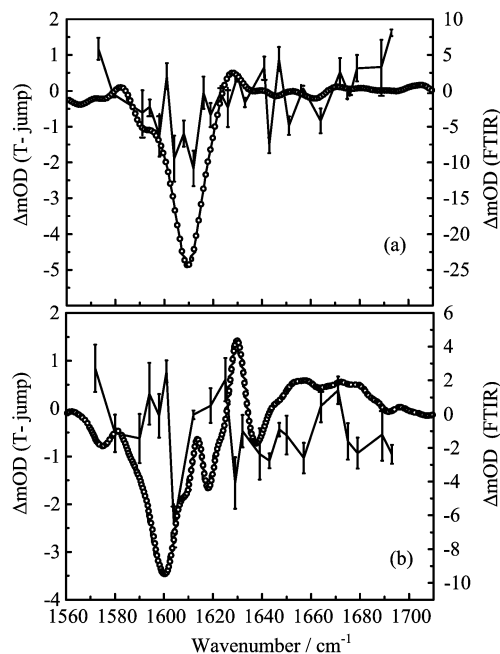


FIG. 4 Comparison of FTIR absorbance difference spectra (open circles) between 20 and 10 °C with the T-jump (from 10 °C to 20 °C) time-resolved IR absorbance difference spectra delayed at 4 μs for (a) histidine and (b) glycine in D₂O.

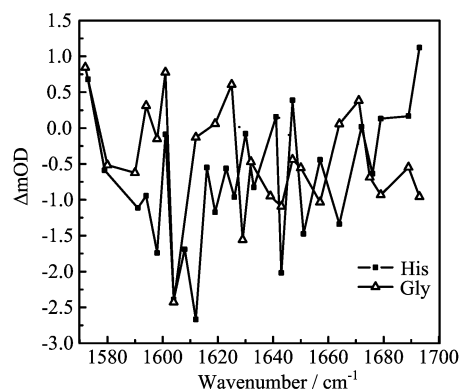


FIG. 5 Comparison of the T-jump (from 10 °C to 20 °C) time-resolved IR absorbance difference spectra delayed at 4 μs of histidine and glycine in D₂O.

tra were acquired. Figure 4 shows the T-jump time-resolved IR absorbance difference spectrum recorded at 4 μs after the T-jump at an initial temperature of 10 °C with a temperature jump of 10 °C. The difference FTIR absorption spectra between 20 and 10 °C are also presented for comparison, which reveals that the time-resolved transient difference IR spectra roughly coincide with the envelope of the difference FTIR spectra. Figure 5 plots the T-jump time-resolved IR difference absorbance spectra of histidine and glycine for comparison. In Fig.5, an intense bleaching peak at 1604 cm⁻¹ for histidine which also appears in the time-resolved

TABLE I Observed Vibrational Frequencies (cm^{-1}) and assignments

	Observed FTIR(T-jump)/ cm^{-1}	Assignment	Literature values/ cm^{-1}	References
Histidine	1407-1402	Symmetric stretching motion of OCO^-	1408	[2,25]
	1617-1620	Asymmetric stretching motion of OCO^-	1619	[2,25]
	1439	CH_3 deformation and CN stretching	1439	[25]
Glycine	1413	Symmetric stretching motion of OCO^-	1413	[2]
	1620	Asymmetric stretching motion of OCO^-	1621	[2]
	1439	CH_3 deformation and C–N stretching	1439	[25]
4-MeIm	1438	CH_3 deformation and C–N stretching	1451	[12]
	1485	N2–C3 stretching	1485	[12]
	1570	C4–C5 stretching	1569	[12]

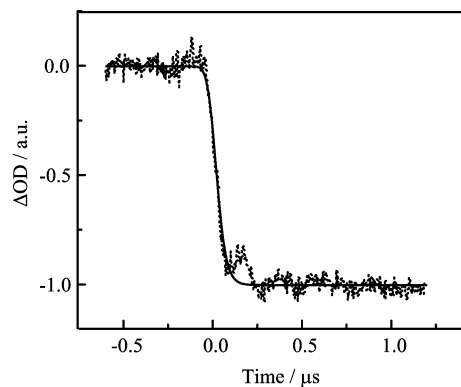


FIG. 6 Kinetics of IR difference absorbance of Histidine at 1604 cm^{-1} in response to a temperature jump from 10°C to 20°C (dotted line), the kinetics is fitted by a mono-exponential expression with a time constant of $30 \pm 10 \text{ ns}$ (solid line).

transient difference absorbance spectrum of glycine is assigned to the COO^- asymmetric vibration. There is another intense bleaching peak located at 1612 cm^{-1} which is absent in the spectrum of glycine. This peak is also in the range of COO^- asymmetric vibration, and can be assigned to the COO^- asymmetric vibration of histidine. The fact suggests that histidine dissolved in D_2O at least has two different carboxyl forms. Figure 6 shows the transient IR absorption kinetics of histidine solution in response to a T-jump of 10°C at an initial temperature of 10°C at 1604 cm^{-1} . The rising phase was fitted by a mono-exponential expression which gives rise to a time constant of $30 \pm 10 \text{ ns}$.

The assignment of the observed bands in both FTIR and the time-resolved IR spectra are summarized in Table I.

The effect of hydrogen bonding on the amino acids vibration spectra can be rationalized by considering the interaction as the formation of intermolecular donor-acceptor pair between the COO^- and NH_3^+ groups, or between the functional groups and water molecules. Such an intermolecular hydrogen bonding can be represented in Fig.1 by an analogy to that between the amide

molecules [27], which shows that a donor-acceptor interaction results in increasing polarity of the bonds between the donor and acceptor atoms. The increasing polarity is related to an increase in the fractional positive charge at the acceptor atoms and an increase in the fractional negative charge at the donor atom. The original loss of the negative charge at the donor atom is overcompensated by attracting the electronic charge from other parts of the donor molecule to the donor atom. In this way the electron density at the donor atom is increased. This has been described as “pile up effect” of the negative charge at the donor atom. The original decrease in the fractional positive charge at the acceptor is also overcompensated by passing over negative charges. In this way the fractional negative charges of other nuclei in the acceptor component are increased. This is the “spill over effect” of negative charge from the acceptor atoms. Both the pile up and spill over effect result in the same electron flow and enhance the effect known as cooperative effect. The electron flowing to more negative atoms results in an increased interatomic distance, while flowing to a less electronegative atom results in a decreased interatomic distance [28].

A change in temperature leads to a change in the intermolecular interaction distance, and consequently a change in the donor-acceptor interaction strength. Therefore at lower temperature, a stronger donor-acceptor interaction, resulting in weaker N–H and C–O and a stronger C–N bonds must be expected. The absorbance is proportional to the square of the transition dipole moment [25]. At a higher temperature the intermolecular hydrogen bond is weakened, giving rise to a blue shift of the COO^- asymmetrical vibration indicating a reduced interatomic distance, and possibly a smaller transition dipole moment. This would lead to a decrease in the absorbance as observed in the experiment.

Based on the above model, two kinds of carboxyl groups can be expected, i.e., one is within the intermolecular chain linked by the intermolecular hydrogen bonds referred as chain carboxyl group; the other is exposing to the solvent forming hydrogen bonds with the solvent molecules referred as end carboxyl group.

Obviously the hydrogen bonding within the chain is stronger than that formed between the carboxyl groups and the solvent molecules. Therefore the asymmetric vibration of COO^- of the former would lie at a lower frequency than the latter. Therefore we assign the two bleaching peaks at 1604 and 1612 cm^{-1} observed in histidine solution to the asymmetric stretching vibration of chain carboxyl group and end carboxyl group respectively. It is interesting to note that the intensities for these two bleaching peaks are almost the same, which indicates that histidine molecules in aqueous solution exist in a dimer-like form linked by intermolecular hydrogen bonds. In contrast, only one bleaching peak at 1604 cm^{-1} corresponding to the asymmetric vibration of COO^- was observed in glycine aqueous solution, which indicates the population of chain carboxyl groups is dominant over that of the end carboxyl groups. The fact reveals that glycine molecules form a longer chain with a number of molecules much larger than two. The intermolecular chains for histidine and glycine are illustrated in Fig.7. For the glycine intermolecular chain, it is possible for it to have a variable length, which would lead to a broad distribution of the IR absorption of the chain COO^- groups. This is consistent with the observation that the FTIR difference absorbance spectrum for glycine between two different temperatures has a much broader spectral width at lower frequency than that at higher frequency as shown in Fig.3(b). To further confirm the above conclusion, we conducted the temperature-dependent FTIR spectra of glycine and histidine at a more acidic D_2O solution by dissolving amino acids into D_2O at a pD value of 1.53. The corresponding FTIR difference absorbance spectra between 20 and 10 $^\circ\text{C}$ are shown in Fig.3(c). In a more acidic solution, more COO^- would be protonated, and this would lead to form shorter glycine intermolecular chains, and consequently causes a blue shift in the absorption spectra of the chain carboxyl groups. In addition a decrease in absorption intensity (bleaching peak) would also be expected in the temperature-dependent FTIR difference spectra compared to those at a neutral pD value. The acidity effect on the absorption peak position and the corresponding bleaching absorbance were confirmed for glycine in Fig.3(c). In contrast the acidity effect only causes the decrease in the difference absorbance intensity (bleaching peak) and almost has no effect on the absorption peak position for histidine. The fact is consistent with that the histidine molecules form a dimer-like intermolecular structure.

After a temperature jump from 10 $^\circ\text{C}$ to 20 $^\circ\text{C}$, a part of the hydrogen bonds are broken accompanied by a decrease in the hydrogen bond strength of the remaining hydrogen bonds. These processes correspond to the rising phase of the IR kinetics in response to the T-jump as shown in Fig.6. The time constant of 30 ± 10 ns fitted for the rising phase is within the temporal resolution limit of our instrument, indicating breaking or weakening the hydrogen bond is a very fast process.

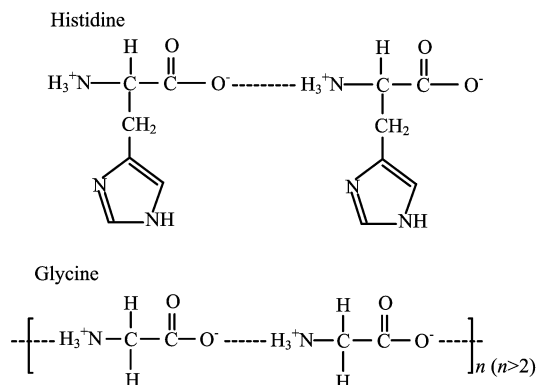


FIG. 7 Schematic diagrams illustrate the intermolecular hydrogen bonds formed in histidine and glycine of different chain length.

IV. CONCLUSION

Temperature-dependent FTIR spectra and T-jump time-resolved IR transient difference spectra of histidine and glycine show that histidine and glycine form intermolecular hydrogen bonds and hydrogen bonds with the solvent molecules in aqueous solutions. Upon heating, the asymmetric vibrations of COO^- with a maximum intensity around 1600-1610 cm^{-1} at lower temperature are blue-shifted, indicating a decrease in the hydrogen bond strength when raising the temperature. Based on the model of intermolecular hydrogen bonding, two types of carboxyl groups are defined. One referred as chain group locates inside the intermolecular chain, the other referred as end group exposes to the environment forming hydrogen bonds with the solvent molecules.

After a temperature jump from 10 $^\circ\text{C}$ to 20 $^\circ\text{C}$, two bleaching peaks at 1604 and 1612 cm^{-1} were observed by the time-resolved IR transient difference spectrum in the histidine D_2O solution, the lower vibration frequency is assigned to the chain COO^- group while the higher frequency is assigned to the end COO^- group since the hydrogen bonds in the former is expected to be stronger than the latter. In addition the intensities of these two bleaching peaks are almost the same. However, in glycine D_2O solution, only the lower frequency at 1604 cm^{-1} bleaching peak has been observed. The fact indicates that histidine forms a dimer-like intermolecular chain in the solution while glycine forms a relatively longer chain varying in chain length in the solution.

The rising phase of the IR absorption kinetics in response to the temperature-jump detected at 1604 cm^{-1} for histidine has a time constant about 30 ± 10 ns, which is within the resolution limit of our instrument, indicating breaking or weakening the hydrogen bond is a very fast process.

V. ACKNOWLEDGMENTS

We thank Prof. Qing-xu Yu and Wang Zhang of Dalian University of Technology for their technical support in CO laser operation. This work was supported by the National Natural Science Foundation of China (No.20373088), the Program for Innovation Group (No.60321002), the Innovative Project of Chinese Academy of Sciences (No.KJ CX2-SW-w29), and the National Key Project for Basic Research (No.2006CB910302).

- [1] H. Torii, T. Tatsumi, T. Kanazawa, and M. Tasumi, *J. Phys. Chem. B* **102**, 309 (1998).
- [2] H. Torii, T. Tatsumi, and M. Tasumi, *J. Raman Spectrosc.* **29**, 537 (1998).
- [3] S. Krimm and J. Bandekar, *Adv. Prot. Chem.* **38**, 181 (1986).
- [4] W. C. Reisdore and S. Krimm, *Biochemistry* **35**, 1383 (1996).
- [5] R. Gilmanshin, S. Williams, R. H. Callender, W. H. Woodruff, and R. B. Dyer, *Biochemistry* **36**, 15006 (1997).
- [6] R. Gilmanshin, S. Williams, R. H. Callender, W. H. Woodruff, and R. B. Dyer, *Proc. Natl. Acad. Sci. (USA)* **94**, 3709 (1997).
- [7] M. Jackson and H. H. Mantsch, *Can. J. Chem.* **69**, 1639 (1991).
- [8] D. Hecht, L. Tadesse, and L. Walters, *J. Am. Chem. Soc.* **115**, 3336 (1993).
- [9] W. W. Wright, M. Laberge, and J. M. Venderkooi, *Biochemistry* **36**, 14724 (1997).
- [10] R. B. Dyer, F. Gai, W. H. Woodruff, R. Gilmanshin, and R. H. Callender, *Acc. Chem. Res.* **31**, 709 (1998).
- [11] R. Callender and R. B. Dyer, *Chem. Rev.* **106**, 3031 (2006).
- [12] K. Hasegawa, T. A. Ono and T. Noguchi, *J. Phys. Chem. B* **104**, 4253 (2000).
- [13] A. A. Hays, I. R. Vassiliev, J. H. Golbeck, and R. J. Debus, *Biochemistry* **37**, 11, 352 (1998).
- [14] T. Noguchi, Y. Inoue, and X. S. Tang, *Biochemistry* **38**, 399 (1999).
- [15] P. A. Frey, S. A. Whitt, and J. B. Tobin, *Science* **264**, 1927 (1994).
- [16] M. Ye, Q. L. Zhang, H. Li, Y. X. Weng, W. C. Wang, and X. G. Qiu, *Biophys. J. BioFAST*: doi10.1529/biophysj.107.106799 (2007).
- [17] Q. L. Zhang, L. Wang, Y. X. Weng, X. G. Qiu, W. C. Wang, and J. X. Yan, *Chin. Phys.* **14**, 2484 (2005).
- [18] W. O. Wray, T. Aida, and R. B. Dyer, *Appl. Phys. B* **74**, 57 (2002).
- [19] T. Wang, Y. Zhu, Z. Getahun, D. Du, C. Y. Huang, W. DeGrado, and F. Gai, *J. Phys. Chem. B* **108**, 15301 (2004).
- [20] C. Y. Huang, Z. Getahun, Y. Zhu, J. W. Klemke, W. F. DeGrado, and F. Gai, *Proc. Natl. Acad. Sci. (USA)* **99**, 2788 (2002).
- [21] S. Y. Venyaminov and N. N. Kalnin, *Biopolymers* **30**, 1243 (1990).
- [22] M. Wolpert and P. Hellwig, *Spectrochim. Acta A* **64**, 987 (2006).
- [23] Y. U. N. Chirgadze, O. V. Fedorov, and N. P. Trushina, *Biopolymers* **14**, 679 (1975).
- [24] A. Wolpert and P. Hellwig, *Spectrochim. Acta A* **64**, 987 (2006).
- [25] A. Barth and C. Zscherp, *Q. Rev. Biophys.* **35**, 369 (2002).
- [26] W. W. Wright and J. M. Venderkool, *Biospectroscopy* **3**, 457 (1997).
- [27] W. Herrebout, K. Clou, H. O. Desseyn, and N. Bleton, *Spectrochim. Acta A* **59**, 47 (2003).
- [28] V. Gutman, *The Donor Acceptor Approach to Molecular Interactions*, New York: Plenum Press, (1978).